Towards Temperature Monitoring in Long-Term Grain Storage

Rastislav Fáber
Faculty of Chemical and Food Technology,
Slovak University of Technology in Bratislava
Bratislava, Slovakia
rastislav.faber@stuba.sk

Richard Valo
Faculty of Chemical and Food Technology,
Slovak University of Technology in Bratislava
Bratislava, Slovakia
richard.valo@stuba.sk

Miloš Roman
Elkora s.r.o.
Bratislava, Slovakia
milos.roman@gmail.com

Radoslav Paulen
Faculty of Chemical and Food Technology,
Slovak University of Technology in Bratislava
Bratislava, Slovakia
radoslav.paulen@stuba.sk

***Abstract*—Long-term grain storage solutions use spacious facilities holding thousands of tons of different commodities. Molds can contaminate the stored grain developing local zones of high temperature, i.e. hot-spots. Continuous temperature monitoring is therefore important to prevent substantial damage to the stored commodities. However, it is hard to do so due to the immense scale and uneven surface of the area of storage. We propose a method that uses surface temperature monitoring by an infrared camera from an autonomous flying drone, cable car, or autonomous grain vehicle. A temperature map with identified anomalous areas will enable timely measures to avert damage to the stored agricultural products. This paper consists in creating a heat-transfer model of the stored grain. For this purpose we constructed and performed a small-scale experiment in the first stage of the presented project. From the collected data, a heat transfer model was identified.**

***Index Terms*—Identification, Sensors, Arduino, Temperature monitoring**

I. Introduction

In today's world, where the human population approaches 8 billion, agriculture plays a critical role in our lives. Modern agriculture enabled people to grow surplus food and thus devote themselves to tasks unrelated to farming. As a result, spacious facilities were allocated for long-term grain storage. They serve as supplies during crop failure or for sale [1]. The agricultural sector provides not only essential daily food for us humans, but also feed for domestic animals and all livestock.

The spoilage risk of stored grain is always present — mainly when the surrounding conditions are extreme. We need to monitor the stored grain constantly. The grain itself is considered a living matter. Respiration combined with its poor heat-conducting ability and possible infestations will most likely lead to the formation of hot-spots — two zones with different temperatures [2].

The hot-spots and their early detection are the main focus of our research. The hot-spots form when the high moisture content is present and the temperatures rises — this often results in mold growth, which further accelerates the whole process of grain spoilage and mycotoxin development. There are multiple other factors making the formation of hot-spots significantly faster by participating in this chain reaction. These links and their impact on grain spoilage are shown in Fig. 1. It depends on the type of stored grain and its constituents (fat, protein, etc.), ambient conditions (temperature, amount of light, humidity, etc.), as well as positive/negative microbial interactions. Furthermore, it is a fact that fungi and pests produce higher amounts of heat compared to the respiration of grain by itself [2], [3].

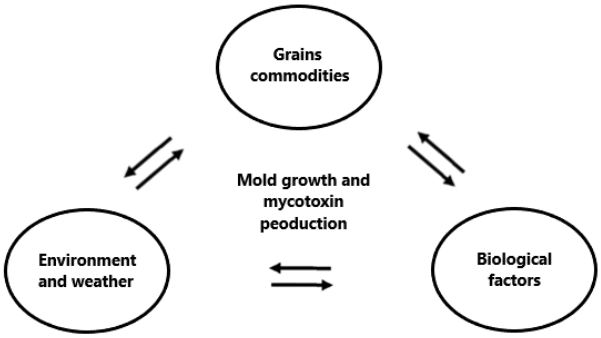

Fig. 1. Illustration of the three main factors affecting the growth rate of fungi and the production of mycotoxins in stored grain and interactions among them [5].

Potential degradation must be detected at the earliest stage possible to prevent heavy losses, as grain deterioration increases exponentially with time [7], [8]. Locating a hot-spot in large storage facilities among tens of thousands of tons of grains is not a straight-forward task. The heat difference just one meter from the centre of a hot-spot can be easily over 10°C. In other words, the grain must be monitored thoroughly so that places with elevated temperatures are not overlooked [9].

As we are mostly interested in bulk storage, we propose an

978-1-6654-8775-7/22/$31.00

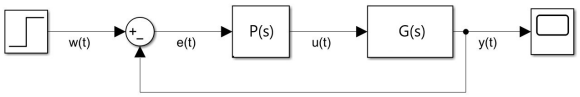

Fig. 2. Illustration of closed-loop feedback control.

automated method of early hot-spot detection in addition to the already proven manual methods for grain monitoring — thermography. As a result of this method, we obtain a thermal map (combination of thermal images of the top layer of grain) on which we can observe the temperature differences — if present, and identify the hot-spots in stored commodities. After the exact location of a hot-spot is unveiled, appropriate action can take place to eliminate this issue.

It is important to control the preservation process so that when the storage period ends, grain has retained as many of the original nutrients as possible [10]. We can obtain a more comprehensive view of the overall condition of stored grains when compared to the currently used methods of (i) *monitoring* — walking through the piles of stored product and randomly inserting a thermometer (probe) into the grain or (ii) *grain sampling* — taking multiple samples, before and during the storage period, for moisture and nitrogen content evaluation.

A more efficient and automated method that would not require human intervention in the process — one that would not directly interfere with the stored commodities — would be a pleasant change for farmers if this method proved to be effective. It is only required to evaluate the data after a temperature map is created, and, if necessary, take additional measures to eliminate the identified hot-spots.

Heat-transfer model identification of stored grain is the goal described in this paper. Firstly, we describe the creation of an artificial hot-spot in Section II used for high-fidelity hardware simulation. The closed-loop identification is then conducted to uncover the dynamical behavior of the heat transfer in the grain bulk in Section III.

II. Hot-spot hardware simulation

To be able to develop and test a temperature monitoring solution, we conduct several lab experiments. To this end, we construct a hot-spot hardware emulator, where we use a heat-generating component to simulate a real-world scenario of hot-spot occurrence. The heat generator has to reliably generate heat under the surface of sunflower seeds for any given reference temperature for long periods of time. Our solution includes dissipating power directly into the grain by using a high-power resistor as a heat sink, therefore increasing the temperature of surrounding seeds. To ensure that the constant temperature is maintained during the duration of the experiment, we implement an automatic closed-loop control.

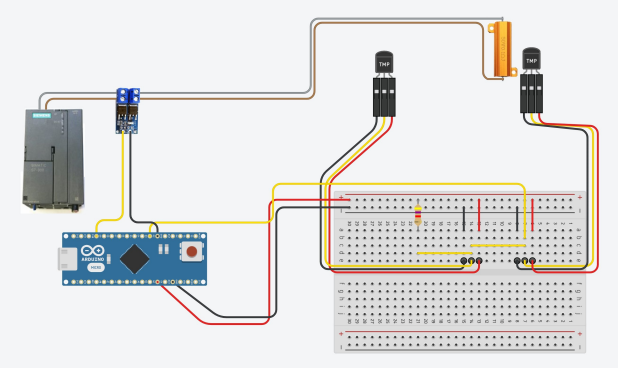

Fig. 3. Hardware for simulating an artificial hot-spot, created with Tinkercad [11].

In control systems, a controller adjusts the control input to reach a desired output in the presence of disturbances. The most popular type of control is PID — which is an acronym for Proportional, Integral, and Derivative. There is no need to maintain the exact value of the setpoint in our experiment, as we monitor the temperature difference on the surface of stored sunflower seeds. Therefore a proportional controller is sufficient. A simplified scheme created in MATLAB Simulink is shown in Fig. 2. The system represented by a transfer function $G(s)$ is controlled by a controller $P(s)$ — computing an action intervention $u(t)$ based on the calculated error $e(t)$ from the output $y(t)$ and the desired reference temperature, $w(t)$ simulated by the step response block (left most).

The high-power resistor is connected to a *Siemens S7* power supply, shown in Fig. 3. For a working solution, a separate microcontroller, *Arduino Nano*, is used in connection with a MOSFET module. We aim for the controller to reduce the voltage as the temperature approaches desired setpoint. To achieve this, the output of the microcontroller must consist of a series of *high* and *low* pulses ("on" and "off"). The digital pulses of regulated voltage are called Pulse-width modulation (PWM). The duty cycle of PWM refers to the *high* pulses when the output signal is active [18].

Finally, to close the loop, a single DS18B20 temperature sensor is attached directly on the body of the high-power resistor with a self-locking nylon cable (zip-tie) with a layer of thermal paste applied between them. By doing so, we ensure accurate temperature readings from the resistor. The other sensor is encapsulated and the overall wiring is identical to the previous example, with the only difference of power input — directly from the Arduino board. After the reference temperature is set and the code is uploaded to the microcontroller, we can turn on the power supply and make sure the behavior of the system meets our predictions in a small-scale experiment.

The implemented code [19], presented in Listing 1, contains the definition for all necessary constants and the main loop for proportional feedback control. We first establish the proportional element (for the controller) and defined the setpoint

Listing 1. Arduino IDE — Proportional control example code.

```
// Controller setup
    float setPoint = 80;
    // Proportional gain tunning parameter
    float Kp = 1;
    // Integral gain tunning parameter
    float Ki = 0;
    // Derivative gain tunning parameter
    float Kd = 0;
    //  e(t) =  setpoint - process variable
    float error = 0;
    float currentTime = 0;
    float previousTime = 0;
    float cumError = 0;
    float elapsedTime = 0;
    float rateError = 0;
    float lastError = 0;
    float output = 0;
// Main loop for artificial hot-spot
void loop() {
  {
  // time
  currentTime = millis();
  elapsedTime = currentTime - previousTime;

  sensors.requestTemperatures();
  // PID
  // P
  error = setPoint - sensors.getTempCByIndex(1);
  // I
  cumError += error * elapsedTime;
  // D
  rateError = (error - lastError)/elapsedTime;
  // eq
  output = Kp * error + Ki * cumError
         + Kd * rateError;
  if(output < .0)
    output = .0;
  if(output > 100.0)
    output = 100.0;
  val = (int)(output*255/100); // set the val
  // analogWrite values from 0 to 255
  analogWrite(ledPin, val);
  // new k
  lastError = error;
  previousTime = currentTime;
  }
}
```

and the output values (to calculate the error). The steady-state control error will be non-zero due to not using an integral part. Tuning of the controller was done experimentally to ensure a non-aggressive and safe behavior of the process.

We use a small, 13.4 × 8.0 × 3.0 centimeter container filled with sunflower seeds and put both — the hot-spot hardware and a secondary DS18B20 sensor under the surface layer with a five centimeter distance between each other (Fig. 4). We added the second temperature sensor to measure transferred heat through the grain over time. The proportional controller starts to lower the voltage when approaching the setpoint and we were reading both temperatures in regular intervals. The simulation ran for over 300 seconds and the behavior of the system was stable. To ensure proper data collection, we used the following shell script to convert them directly from the Arduino IDE serial monitor into a matrix form.

Listing 2. Shell script — Data conversion example.

```
#!/bin/bash
echo "Sensors=[">b.txt
cat a.txt | sed 's/ -> //1' | sed 's/:/*60+/1' \
   | sed 's/:/)*60+/1' | sed 's/^/(/1' >> b.txt
echo "]">>b.txt
```

Fig. 4. The first test of hardware for simulating an artificial hot-spot — covered with grain during the duration of the experiment.

A small-scale experiment was conducted. A self-made, resistor-based regulated heat source was placed into a small plastic container filled with sunflower seeds and three temperature sensors. One sensors was directly attached on the heat source, one at a distance from the heat source, and one outside the container to measure ambient temperature. The whole setup is shown in Figure 3 and the seed box is presented in Fig. 4.

III. Closed-loop Identification

The data obtained from the experiment are shown in Fig. 5. The first graph represents the results of the reference temperature tracking of the heat source, where we can observe the expected steady-state offset from the reference. The second graph shows the corresponding control action ($u(t)$) of the proportional controller. The bottom graph shows a (slight) increase in the grain temperature as a response to the hot-spot generation. The temperature measurements take quantized values due to the minimal resolution of the DS18B20 temperature sensor i.e., 0.0625°C.

Although a series of open-loop step tests is a common practice in today's automatic control industry, we chose a different approach. Closed-loop identification is a method of identifying a model, where the process is fully or partially regulated by a feedback controller [12]. In our case, we assume a first-order system, regulated in a closed loop with a proportional controller — this connection is shown in Fig. 2, where $G(s)$ represents the dynamic transfer function. Our controller design successfully stabilized and regulated the system. The transfer

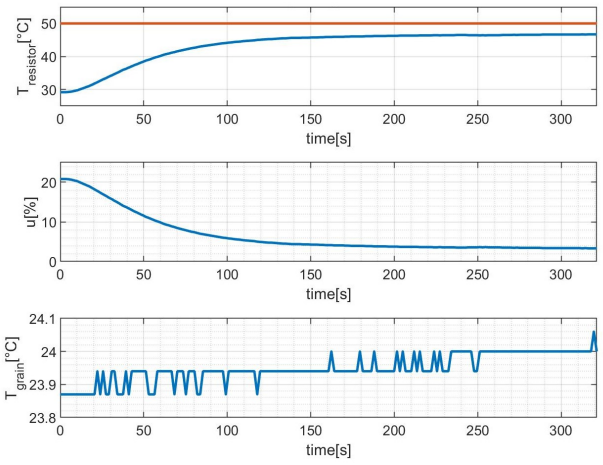

Fig. 5. Closed loop temperature control - collected data.

TABLE I
IDENTIFIED PARAMETER VALUES.

	Closed-Loop System	Open-Loop System
Static Gain	0.9	7.0
Time Constant	60.7	485.4

function of the closed-loop can be defined as follows.

$$G_{cl}(s) = \frac{K_R G(s)}{1 + K_R G(s)} = \frac{K_R \frac{K}{Ts+1}}{1 + K_R \frac{K}{Ts+1}} = \\ = \frac{K_R K}{Ts + K_R K + 1} = \frac{\frac{K_R K}{K_R K+1}}{\frac{T}{K_R K+1} s + 1} = \frac{K_{cl}}{T_{cl} s + 1}, \quad (1)$$

where the subscript cl represents constants associated to the closed loop, the subscript R represents constants associated to the controller (regulator), and K and T represent the static gain and the time constant of the process, respectively.

Closed regulation loop — modified expression:

$$G_{cl}(s) = \frac{K_{cl}}{T_{cl} s + 1}. \quad (2)$$

All needed parameters for the closed-loop model can be obtained from the derived transfer function. Because the controller is present, static gain is calculated differently to a open-loop system. We derive it as a ratio of the difference in output to the difference in reference signal.

$$K_{cl} = \frac{\Delta y}{\Delta w}. \quad (3)$$

We can computed all the parameters derived from the transfer function. The time constant is calculated from the denominator and its value is estimated by least-squares regression using the measured data. Similarly, static gain is calculated from the numerator.

$$K_{cl} = \frac{K_R K}{K_R K + 1}, \qquad T_{cl} = \frac{T}{K_R K + 1}. \quad (4)$$

We state the estimated parameters of the both closed and open-loop systems in Tab. I. The static gain of the Closed-loop shows, that we can achieve 90% of the set-point. This fact also confirms the presence of a steady-state control error because the integral part of a PID controller was not implemented. The static gain of the open-loop system basically represents the ease with which the input can initiate a change on the output from an initial condition — a new steady state after the action intervention. The time constant difference is significant, and this result was expected. It represents faster behavior of the regulated system for achieving the set-point. In conclusion, we were satisfied with how the system behaved, there was no need to achieve an exact set-point, so the proportional control was sufficient.

IV. ACHIEVED RESULTS

The small-scale experiment was successful as we obtained results that can be expected, and the methods we used proved to be suitable. Furthermore, we decided to assemble a mathematical model to ensure the reproducibility and verifiability of our results — to simulate the overall heat transferred by conduction. To do so, we derived and solved two differential equations

$$\frac{\mathrm{d}T_r}{\mathrm{d}t} = \frac{K_{cl}\Delta w - T_r}{T_{cl}}, \quad (5)$$

where T_r represents resistor temperature, i.e., system output in Eq. (3). This equation is derived from the experimentally identified first-order open-loop transfer function. It represents the estimated temperature of the resistor over a time period. The second equation reads as

$$m_g c_p \frac{\mathrm{d}T_g}{\mathrm{d}t} = \frac{\lambda_{r\to g} A_{r\to g}}{\delta_{r\to g}} (T_r - T_g), \quad (6)$$

which represents the estimated heat on the DS18B20 temperature sensor placed in the grain (heat transfer from the resistor to the grain, $r \to g$). It is derived based on Fourier's law of heat conduction — heat transfer rate is proportional to the difference in temperature (grain $\leftrightarrow$ hot-spot) and the cross-sectional area, and inversely proportional to the distance from the hot-spot to the measured point in grain (thickness of the grain layer) [13], [14]. We considered a homogeneous environment and neglected the influence of ambient temperature. The subscript g represents the grain, m represents the weight of one grain approximated as $0.05667\,\mathrm{g}$, c_p represents the specific heat capacity of sunflower seeds as $c_p = 5.2750\,\mathrm{kJ\,kg^{-1}\,K^{-1}}$ [15], λ represents the thermal conductivity of sunflower seeds as $\lambda = 0.0859\ \mathrm{W.m^{-1}\,K^{-1}}$ [15], A represents the approximated cross-sectional area of one sunflower seed, measured as $1 \times 0.45\,\mathrm{cm}$ (comparable with other studies [16]), and δ represents the distance (thickness) of $5\,\mathrm{cm}$ the heat transferred between the resistor (higher temperature T_r) and the temperature sensor (lower temperature T_g).

Using MATLAB's *dsolve* function, we obtained a very similar behavior — a behavior that described reality very well

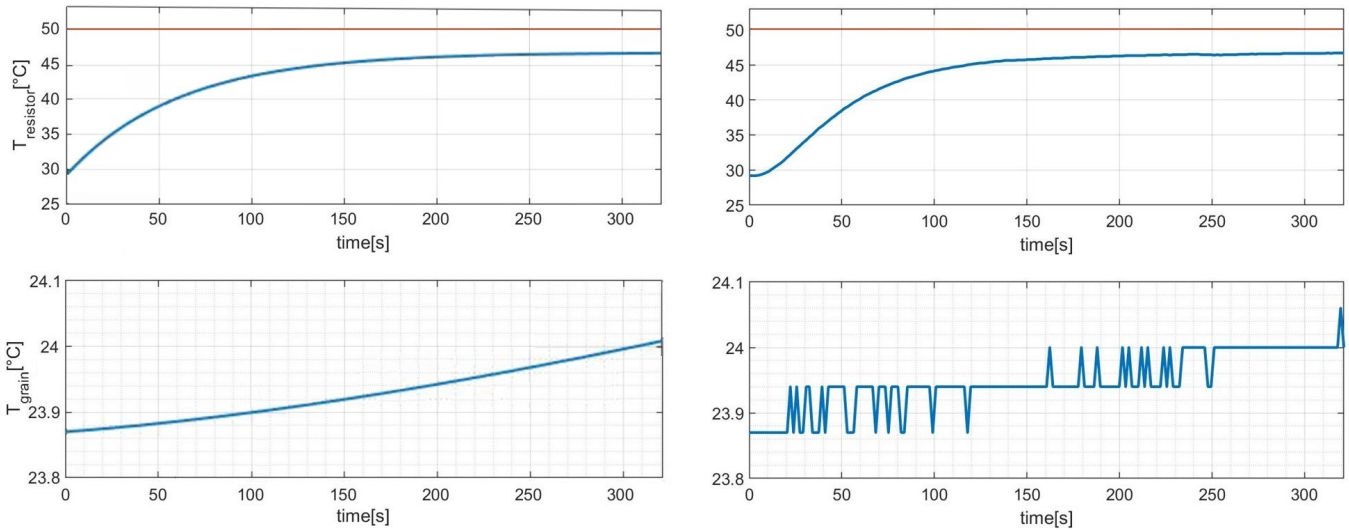

Fig. 6. The comparison of data for heat transfer estimate (left) and closed-loop temperature control (right).

(Figure 6). The first row represents the temperature from the resistor, the estimated behavior (on the left) is almost equivalent to the real process (on the right). The Root Mean Squared Error value (RMSE) was calculated as 0.8017 — where 0 represents identical behavior.

$$\text{RMSE} = \sqrt{\frac{1}{N}\sum_{i=1}^{N}(y_{\text{data},i} - y_{\text{sim},i})^2}, \tag{7}$$

where y_{data} and y_{sim} represent measured data and calculated model predictions, respectively.

The bottom plot shows the influence of the heat source on the surrounding grain over time. We can see that the calculated curve (on the left) and the real process (on the right) would be almost alike. The correct choice of parameters in Eq. (6) was important. The associated constants for black sunflower seeds that were used in the calculations were averaged from similar experiments and did not fully correspond to the grain used in our experiments. Furthermore, the approximation depends heavily on the moisture content and the seed density of black sunflower seeds.

A. Discussion

Many experts working in grain warehouses consider temperature probing as an irreplaceable method, as no one has yet come up with a more reliable monitoring method. Although, we presented obtained results as applicable and confirm that we can efficiently identify hot-spots autonomously by mapping stored grain commodities with a thermal imager, there is always room for improvement. Multiple ideas for an improved design phase come to mind. They would include a pouch of some sort to improve the connection between the high-power resistor and temperature sensor instead of a singular zip-tie. A 3D printer for creating a firm "cage" to better support the hardware including both used microcontrollers, with the circuit board and breadboard, so they would have their designated place not risking possible connection issues. Furthermore, several steps could be taken to improve the results achieved. We could devote more time to simulations to more accurately describe the heat transfer from the artificial hot-spot so it would reflect the real-world behavior. This would include mathematically describing the individual zones around the hot-spot and their effect on heat transfer, as well as implementing the approximate shape of the high-power resistor. In addition, taking the time to test the effectiveness of the thermal imager in identifying hot-spots located deeper under the surface layer would be beneficial as well. From our further findings, not presented in this article due to space limitations, a hot-spot located ten centimeters under the surface (80°C) is detected by the thermal imager after approximately one hour of development. However, the size, temperature, depth, or other variables of a hot-spot may differ depending on the storing conditions in a facility. Moreover, we focused on a simple practical and easily reproducible solution. Yet, if we were considering an alternative higher-cost solution, more suitable thermal cameras and UAVs can be tested. For example, using and modifying hardware intended for similar uses as *flyability' Elios 2* [17], an indoor drone for confined space inspections. The grains are often filled up to the ceiling of the storage hall with minimal space to maneuver. Further study of this subject would involve developing a software which would use the *Indoor Positioning System* (IPS) as a basis for controlling the movement of an autonomous drone. Creating a proper mobile application for additional calibration and setting of the desired routes would be also necessary.

V. Conclusions

In this paper, we initiated a complex project that has several aspects and is extremely important in modern agriculture. We have studied the current possibilities of grain storage, associ-

ated complications and commonly used approaches on how to solve them in real-world conditions. We programmed reliable temperature control and developed functional hardware which provided us with a source of useful data. We derived mathematical models to run simulations, which confirmed that we were moving in the right direction by calculating comparable results. We implemented commonly used and verified methods into our work, which can be further adjusted to achieve optimal results and can be used for further analyses and simulations. In future articles we will present successful tests of thermal imaging method in a storage facility and prove that even a low-cost approach can successfully detect any minor temperature difference on the top-most layer of grain, and thus reveal a hot-spot.

ACKNOWLEDGMENTS

Authors are grateful to Mag. Martin Kráčmar (Executive Manager of SCHAUMANN SLOVENSKO, spol. s r.o.) and to Matt Swinn (Marketing Manager of Martin Lishman Ltd., United Kingdom) for their time devoted to discussions on the issues related to grain storage. Authors would also like to thank Ing. Vojtech Szabó from Agrosid, a.s., for his willingness to explain the operation process of grain storage, for making warehouses in Gabčíkovo available for testing, and for donating crop seeds for the experiments.

This research is funded by the Slovak Research and Development Agency under the projects APVV-20-0261 and APVV APVV-21-0019, by the Scientific Grant Agency of the Slovak Republic under the grants VEGA 1/0691/21 and VEGA 1/0297/22, and by the European Commission under the grant no. 101079342 (Fostering Opportunities Towards Slovak Excellence in Advanced Control for Smart Industries).

REFERENCES

[1] Kim Rutledge et al., The Art and Science of Agriculture, 2011, Available at https://www.nationalgeographic.org/encyclopedia/agriculture/

[2] OPIsystems, Watch Your Grain: You May Have a Hotspot, 1-2, 2017, Available at https://advancedgrainmanagement.com/learn-grain-management/#grainmanagement

[3] H.A.H. Wallace and R.N. Sinha, Fungi Associated with Hot Spots in Farm Stored Grain, Canadian Journal of Plant Science, 42, 1962

[4] Kane Dane, Why is Agriculture Important and its Role in Everyday Life, Available at https://agriculturegoods.com/why-is-agriculture-important/ 7-4-2022

[5] M. Mannaa and D.K. Kim, Influence of Temperature and Water Activity on Deleterious Fungi and Mycotoxin Production During Grain Storage, Mycobiology, 45 (4), 240, 2017

[6] Demis Esuyawkal and Yenewa Workineh Moshe Kostyukovsky and Anatoly Trostanetsky and Elazar Quinn, Review on major storage insect pests of cereals and pulses, Asian Journal of Advances in Research, 63, 41–56 7 - 16, 2022 2016, Available at http://www.mbimph.com/index.php/AJOAIR/article/view/2736 Available at https://brill.com/view/journals/ijps/63/1/article-p7_3.xml

[7] Hall D.W., Handling and Storage of Food Grains in Tropical and Subtropical Areas, Food & Agriculture Org., 156, 1970

[8] Moshe Kostyukovsky and Anatoly Trostanetsky and Elazar Quinn, Novel approaches for integrated grain storage management, Israel Journal of Plant Sciences, 63, 7 - 16, 2016, Available at https://brill.com/view/journals/ijps/63/1/article-p7_3.xml

[9] MARTIN COBBALD Dealey Environmental, WHERE DO HOT SPOTS IN GRAIN COME FROM?, Available at https://www.dealey.co.uk/blog/where-do-hot-spots-in 22-4-2021

[10] Melkamu Bezabih Yitbarek and Birhan Tamir, Silage Additives: Review, Open Journal of Applied Sciences, 4, 258-274, 2014, Available at https://www.scirp.org/journal/paperinformation.aspx?paperid=44897

[11] Autodesk Inc. TinkerCAD, A free-of-charge online 3D modeling program. Web. Creative Commons., Available at https://www.tinkercad.com

[12] Yucai Zhu Firmin Butoyi, Multivariable and Closed-Loop Identification for Model Predictive Control, 2021, Available at http://www.taijicontrol.com/closelp1.pdf

[13] Azadeh Shahidian and Majid Ghassemi and Javad Mohammadi and Mohadeseh Hashemi, Bio-Engineering Approaches to Cancer Diagnosis and Treatment, 1 - Introduction, 1-22, 2020

[14] Majid Ghassemi and Majid Kamvar and Robert Steinberger-Wilckens, Fundamentals of Heat and Fluid Flow in High Temperature Fuel Cells, Chapter 5 - Fundamental of heat transfer, 101-124, 2020

[15] Ewa ROPELEWSKA Krzysztof J. JANKOWSKI Piotr ZAPOTOCZNY and Bożena BOGUCKA, Thermophysical and chemical properties of seeds of traditional and double low cultivars of white mustard, Zemdirbyste-Agriculture, 105, 257–264, 2018, Available at http://www.zemdirbyste-agriculture.lt/wp-content/uploads/2018/08/105_3_str33.pdf

[16] Esref Isik and Nazmi Izli, Physical Properties of Sunflower Seeds (Helianthus annuus L.), International Journal of Agricultural Research, 2, 677-686, 2007

[17] FLYABILITY, ELIOS 2 — INTUITIVE INDOOR INSPECTION, Available at https://www.flyability.com/elios-2

[18] CADENCE PCB SOLUTIONS, Pulse Width Modulation (PWM) vs DC Voltage and Voltage Control Circuits, Available at https://resources.pcb.cadence.com/blog/2020-pulse-width-modulation-pwm-vs-dc-voltage-and-voltage-control-circuits

[19] Roland Pelayo, Arduino PID Control Tutorial, Available at https://www.teachmemicro.com/arduino-pid-control-tutorial/ INSPECTION, Available at https://www.flyability.com/elios-2